International Journal of Environmental Sciences
ISSN: 2229-7359
Vol. 11 No. 14s, 2025
https://www.theaspd.com/ijes.php

Stochastic And Climate-Driven Modeling Of Malaria Transmission In Rwanda: A Vector-Human Interaction Approach

Carine Frieda Idani[1], Jane Aduda[2], Simon Karanja[3*]

[1*]Department of Mathematics, Pan African University Institute for Basic Sciences, Technology and Innovation, Hosted at Jomo Kenyatta University of Agriculture and Technology, Nairobi, P.O. Box 62000-00200, Kenya
[2]Department of Statistics and Actuarial Science, Jomo Kenyatta University of Agriculture and Technology, Nairobi, Kenya
[3]College of Health Sciences, Jomo Kenyatta University of Agriculture and Technology, Nairobi, Kenya.

Abstract
Malaria transmission depends heavily on climate conditions such as temperature and rainfall, which influence mosquito development and parasite growth. In this study, we build a stochastic model to better understand how these environmental factors affect the spread of malaria over time. The model includes temperature- and moisture-sensitive biological parameters and uses daily climate data from Rwanda. Using numerical simulations based on the Milstein scheme, we explore how mosquito population dynamics and malaria in- fections respond to seasonal changes. Results show that transmission slows down during dry periods, with lower survival and slower mosquito cycles. In some cases, transmission can fade out completely. Mathemati- cally, we verify that the model satisfies Hörmander's condition, supporting the existence of a smooth density and ensuring the system's well-posedness. Spatial maps further highlight how local climate affects malaria risk across regions. This model offers a flexible framework for climate-informed malaria control planning, especially in the face of environmental variability and climate change.

Keywords: *Stochastic modeling, Hormander condition, mosquito lifecycle, mosquito dynamics.*

1. Introduction

Malaria is an infectious disease caused by parasites of the Plasmodium genus and transmitted to humans through the bite of infected female Anopheles mosquitoes. Among over 50 species capable of transmitting the disease, only five Plasmodium species are known to infect humans: P. falciparum, P. vivax, P. malariae, P. ovale, and P. knowlesi [1]. In sub-Saharan Africa, most malaria-related deaths are attributed to P. falciparum, primarily transmitted by Anopheles gambiae and Anopheles arabiensis [2].

According to the World Health Organization, an estimated 263 million malaria cases occurred in 2023, with an incidence of 60.4 cases per 1,000 people at risk up from 58.6 the previous year. The African region continues to bear the highest burden, accounting for 94% of global cases and 95% of malaria-related deaths [3]. Over the years, control efforts have largely relied on insecticide-treated nets (ITNs) and indoor residual spraying (IRS) [4]. However, these strategies face growing challenges such as insecticide resistance.

In parallel, climate change is increasingly recognized as a key driver of malaria dynamics. Changes in temperature, rainfall, and humidity influence both mosquito development and the extrinsic incubation period of the parasite, thereby shaping the spatial and temporal patterns of transmission [4]. Understanding how environmental variability affects malaria risk is essential for anticipating outbreaks and designing effective interventions.

Mathematical modelling has long played a critical role in malaria research. Ross first established the relationship between mosquito density and disease prevalence through deterministic models [5], later expanded by Macdonald, who introduced key metrics like the basic reproduction numberR_0 [6]. These early models provided a foundation for evaluating control strategies and remain influential in public health planning [7, 8, 9]. While these models offer analytical tractability and insight into equilibrium behavior, they often

International Journal of Environmental Sciences
ISSN: 2229-7359
Vol. 11 No. 14s, 2025
https://www.theaspd.com/ijes.php

assume homogeneity across populations and environments, and may not capture local variations or random fluctuations that occur in real settings.

Stochastic modelling was developed to overcome some of these limitations by introducing random perturbations into transmission parameters. These models allow for more realistic simulations, especially in low-transmission settings or areas affected by climate variability [10]. In Yunnan, China, a stochastic model demonstrated how environmental noise in mosquito populations and transmission rates can significantly im- pact malaria persistence and control [11]. Other researchers have included stochastic delays to represent parasite incubation periods in both mosquito and human hosts [12], while some frameworks integrate L´evy noise to account for more abrupt environmental disturbances [13].

However, despite these advances, many stochastic models still treat space and climate as fixed or sec- ondary features. Most frameworks either assume parameter homogeneity across regions or consider noise independently of geographic variability. This limits their applicability in regions like sub-Saharan Africa, where malaria transmission is highly sensitive to spatial heterogeneity in elevation, rainfall, temperature, and human settlement. For instance, malaria risk is typically lower in highland areas due to cooler temperatures that slow mosquito development and parasite maturation, while lowland regions with prolonged rainy seasons can sustain year-round transmission.

To address this gap, this study proposes a stochastic malaria transmission model that incorporates climate-driven biological parameters and allows spatial variation using real climatic data. The model integrates temperature and rainfall dependent functions to regulate mosquito recruitment, development, and survival, thereby capturing seasonal and geographic variations in transmission risk. Mathematically, the model satisfies H ̈ormander's condition—a property that ensures smooth density for the system and supports well posedness in noisy, multidimensional settings.

Numerical simulations are conducted using the Milstein scheme and climate data from Rwanda. The model is used to explore long-term transmission dynamics under stochastic fluctuations, to evaluate extinction and persistence conditions, and to generate spatial maps of key parameters such as recruitment rate and survival probabilities.

2. Methods

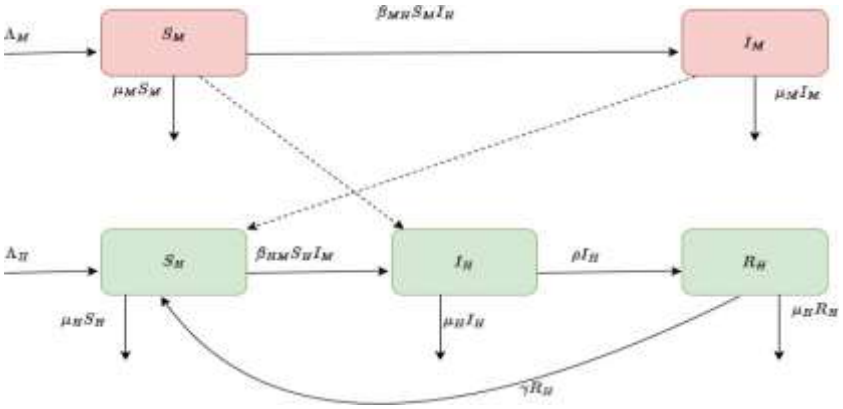

Figure 1: Compartmental diagram of the vector-host interaction.

2.1. The Base Vector-Host Model

We consider a classical host-vector malaria transmission model, where the human population is divided into three compartments.

- $S_H(t)$: susceptible humans,
- $I_H(t)$: infected humans,
- $R_H(t)$: recovered humans.

The mosquito (vector) population is divided into two compartments:

- $S_M(t)$: susceptible mosquitoes,
- $I_M(t)$: infected mosquitoes.

International Journal of Environmental Sciences
ISSN: 2229-7359
Vol. 11 No. 14s, 2025
https://www.theaspd.com/ijes.php

The total human population is $N_H = S_H + I_H + R_H$, and the total mosquito population is $N_M = S_M + I_M$.
The disease spreads from infected mosquitoes to susceptible humans and vice versa. Recovered humans may lose immunity and return to the susceptible class.
The deterministic dynamics of the system are described by the following differential equations:

$$\frac{dS_H}{dt} = \Lambda_H - \frac{\beta_H S_H I_M}{N_H} - \mu_H S_H + \omega R_H$$
$$\frac{dI_H}{dt} = \frac{\beta_H S_H I_M}{N_H} - (\gamma + \mu_H) I_H$$
$$\frac{dR_H}{dt} = \gamma I_H - (\mu_H + \omega) R_H$$
$$\frac{dS_M}{dt} = \Lambda_M - \frac{\beta_M S_M I_H}{N_H} - \mu_M S_M$$
$$\frac{dI_M}{dt} = \frac{\beta_M S_M I_H}{N_H} - \mu_M I_M$$

Table 1: Parameters of the deterministic model and their descriptions

Parameter	Description
Λ_H	Birth rate of humans
Λ_M	Birth rate of mosquitoes
μ_H	Natural death rate of humans
μ_M	Natural death rate of mosquitoes
β_H	Transmission rate from infected mosquitoes to human
β_M	Transmission rate from infected humans to mosquito
ρ	Recovery rate of infected humans
γ	Rate of loss of immunity of humans

2.2. The Stochastic Model and Numerical Scheme

To account for environmental variability in malaria transmission, we extend the deterministic model to a stochastic system by introducing white-noise perturbations into some key rates. These perturbations reflect random fluctuations, such as climatic variations or unpredictable changes in mosquito–human contact patterns.

The definitions of all model parameters are summarized in Table 2.
The resulting stochastic system is formulated using Itô stochastic differential equations (SDEs) as follows:

$$dS_M = [\Lambda_M - \beta_{MH} S_M I_H - \mu_M S_M]\, dt + \sigma_{SM} S_M\, dW_1 \quad (1)$$
$$dI_M = [\beta_{MH} S_M I_H - \mu_M I_M]\, dt + \sigma_{IM} I_M\, dW_2 \quad (2)$$
$$dS_H = [\Lambda_H - \beta_{HM} S_H I_M - \mu_H S_H + \gamma R_H]\, dt + \sigma_{SH} S_H\, dW_3 \quad (3)$$
$$dI_H = [\beta_{HM} S_H I_M - (\mu_H + \rho) I_H]\, dt + \sigma_{IH} I_H\, dW_4 \quad (4)$$
$$dR_H = [\rho I_H - (\mu_H + \gamma) R_H]\, dt + \sigma_{RH} R_H\, dW_5 \quad (5)$$

Symbol	Description
β_{MH}	Transmission rates from infected humans to mosquitoes.

σ_{SM}, σ_{IM}	Diffusion coefficients for stochasticity in S_M and I_M .
W_1, W_2	Independent Wiener processes.
β_{HM}	Transmission rate from infected mosquitoes to humans.
ρ	Recovery rate of infected humans.
γ	Rate of loss of immunity from the recovered population.
$\sigma_{SH}, \sigma_{IH}, \sigma_{RH}$	Diffusion coefficients for stochasticity in $S_H, I_H, and\ R_H$.
W_3, W_4, W_5	Independent Wiener processes.

Table 2: Definitions of parameters and variables for the stochastic model.

To numerically approximate the solutions of this system, we apply the Milstein scheme, which provides improved accuracy over the Euler-Maruyama method when the diffusion term is non-linear.
For a general scalar SDE of the form:

$$dXt = f(Xt)\,dt + g(Xt)\,dWt,$$

The Milstein approximation is given by:

$$X_{n+1} = X_n + f(X_n)\Delta t + g(X_n)\Delta B_n + \frac{1}{2}g(X_n)g'(X_n)[(\Delta B_n)^2 - \Delta t]$$

Where:

- ΔB_n is a Brownian increment over time step Δt,
- $g'(X_n)$ is the derivative of the diffusion function g with respect to X.

This scheme is applied component-wise to the stochastic malaria system, with initial conditions and parameter values specified in the simulation section.

2.3. Positivity of the system

Proposition 2.1. The stochastic system given by

$$dS_M = [\Lambda_M - \beta_{MH}S_M I_H - \mu_M S_M]\,dt + \sigma_{SM}S_M\,dW_1,$$
$$dI_M = [\beta_{MH}S_M I_H - \mu_M I_M]\,dt + \sigma_{IM}I_M\,dW_2,$$
$$dS_H = [\Lambda_H - \beta_{HM}S_H I_M - \mu_H S_H + \gamma R_H]\,dt + \sigma_{SH}S_H\,dW_3$$
$$dI_H = [\beta_{HM}S_H I_M - (\mu_H + \rho)I_H]\,dt + \sigma_{IH}I_H\,dW_4$$
$$dR_H = [\rho I_H - (\mu_H + \gamma)R_H]\,dt + \sigma_{RH}R_H\,dW_5$$

remains strictly positive for all time, provided the initial conditions satisfy $S_M(0), I_M(0), S_H(0), I_H(0), R_H(0) >$
0.
See Appendix Appendix A for the detailed proofs.

2.4. Stability Analysis

Theorem 2.2. The equilibrium points of the stochastic epidemic model are locally asymptotically stable if all eigenvalues of the Jacobian matrix have negative real parts. Furthermore, global stability can be established using a suitable Lyapunov function.
See Appendix Appendix A for the detailed proofs.

2.5. Reproduction number R_0

The basic reproduction number, denoted by R_0, is defined as the expected number of secondary infections

produced by a single infected individual in a fully susceptible population. It serves as a threshold parameter: the disease tends to die out if $R_0 < 1$ and can spread if $R_0 > 1$[14].

For the deterministic malaria model described in subsection 2.1, the basic reproduction number R_0 is given by:

$$R_0 = \sqrt{\frac{\beta_h \beta_v N_v}{(\gamma + \mu_h)\mu_v N_h}}$$

For the deterministic malaria model described in subsection 2.1, the disease-free equilibrium (DFE) is locally asymptotically stable if $R_0 < 1$ and unstable if $R_0 > 1$.

2.6. Extinction of the disease

Theorem 2.3. Consider the stochastic malaria model where the infected human population $I_H(t)$ evolves according to the equation

$$dI_H(t) = [\beta_{HM} S_H(t) I_M(t) - (\mu_H + \rho) I_H(t)]\, dt + \sigma_{IH} I_H(t)\, dW_t$$

Assume that there exists a constant $\delta > 0$ such that: $\frac{S_H(t) I_M(t)}{I_H(t)} \leq \delta \quad \text{for all } t \geq 0,$

and that the noise intensity satisfies: $\frac{1}{2}\sigma_{IH}^2 > (\mu_H + \rho) - \beta_{HM}\delta.$

Then the solution $I_H(t)$ tends to zero exponentially almost surely. More precisely, there exists $\lambda > 0$ such that: $lim\ sup_{t\to\infty} \quad \frac{1}{t} ln\, I_H(t) \leq -\lambda, \quad \text{almost surely.}$

See Appendix Appendix A for the detailed proofs

2.7. Stationary

Theorem 2.4. Existence of Stationary Distribution Let the stochastic system be given by

$$dX(t) = b(X)\, dt + G(X)\, dW(t), \quad X \in R_+^5,$$

with

$$X = \begin{pmatrix} S_M \\ I_M \\ S_H \\ I_H R_H \end{pmatrix}$$

$$b(X) = \begin{pmatrix} \Lambda_M - \beta_{MH} S_M I_H - \mu_M S_M \\ \beta_{MH} S_M I_H - \mu_M I_M \\ \Lambda_H - \beta_{HM} S_H I_M - \mu_H S_H + \gamma R_H \\ \beta_{HM} S_H I_M - (\mu_H + \rho) I_H \rho I_H - (\mu_H + \gamma) R_H \end{pmatrix}$$

$$G(X) = \text{diag}(\sigma_{SM} S_M,\ \sigma_{IM} I_M,\ \sigma_{SH} S_H,\ \sigma_{IH} I_H,\ \sigma_{RH} R_H)$$

Then the system admits at least one stationary distribution in R_+^5 .
See Appendix Appendix A for the detailed proofs.

2.8. Ergodicity

Theorem 2.5. Ergodicity via H ̈ormander's Condition Let the stochastic system be given by

$$dX = b(X)\, dt + G(X)\, dW, \quad X \in R_+^5,$$

where G(X) is diagonal with non-zero entries on $R_+^5 \setminus \{0\}$,and $b(X)$ is smooth. Then the process admits a unique stationary distribution and is ergodic.

International Journal of Environmental Sciences
ISSN: 2229-7359
Vol. 11 No. 14s, 2025
https://www.theaspd.com/ijes.php

See Appendix Appendix A for the detailed proofs.

2.9. Spatial and climatic considerations.

Although the model is not spatially structured in its mathematical formulation, spatial variation is incorporated indirectly through climate-sensitive parameters. Specifically, temperature and rainfall data from different geographic regions are used to adjust key biological and epidemiological rates, such as mosquito recruitment, biting frequency, and parasite development. This approach allows the model to reflect spatial heterogeneity in transmission potential without explicitly modelling spatial compartments or movement. By doing so, it becomes possible to generate spatial maps of transmission-relevant parameters and explore how local environmental conditions modulate malaria risk across regions.

3. Results

3.1. Simulation of the model and validation

To validate the model's theoretical properties and illustrate its biological realism, we conducted several numerical simulations under different stochastic and climatic conditions using the Milstein scheme. All scenarios confirmed the model's ability to reproduce key transmission dynamics while maintaining bounded, biologically feasible trajectories.

Figure 2 presents a representative simulation outcome incorporating stochastic noise and climate-driven variation in the mosquito birth rate Θ_M . The trajectories capture the evolution of malaria indicators such as infection prevalence, incidence,Rapid Diagnostic Test (RDT) positivity, and Entomological Innoculation Rate (EIR) over time. Peaks and troughs reflect the influence of environmental variability, while the synchrony between indicators confirms model consistency. These results validate the robustness of the model and support its relevance for climate-sensitive intervention planning.

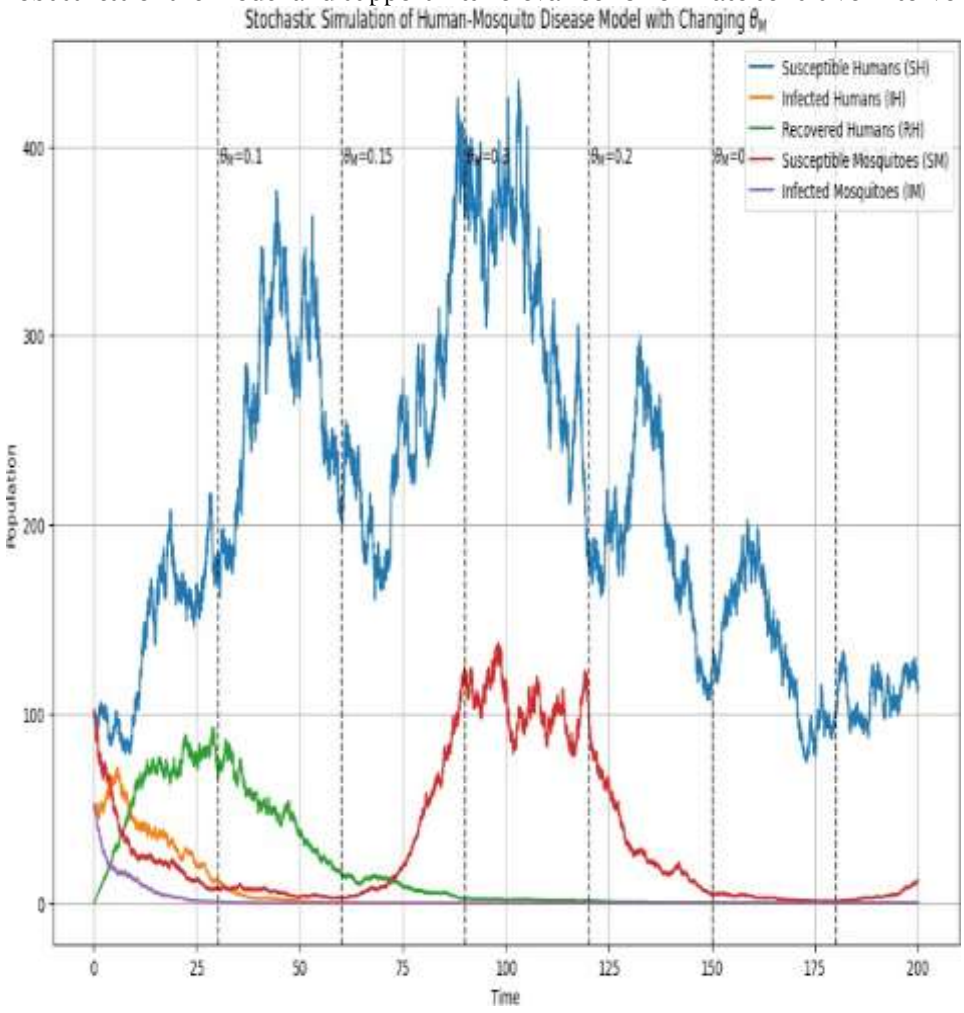

Figure 2: Representative stochastic simulation of the malaria model under environmental variability. The dynamics reflect the temporal evolution of key indicators: prevalence, incidence, RDT positivity, and EIR under varying mosquito birth rates θ_M.

3.2. Spatial analysis

The climate data used in this study come from ERA5, CHIRPS, and climate model projections from CMIP5 and CMIP6, covering the period from 1988 to 2035. Administrative boundary shapefiles used for spatial mapping were obtained from the National Institute of Statistics of Rwanda (NISR).

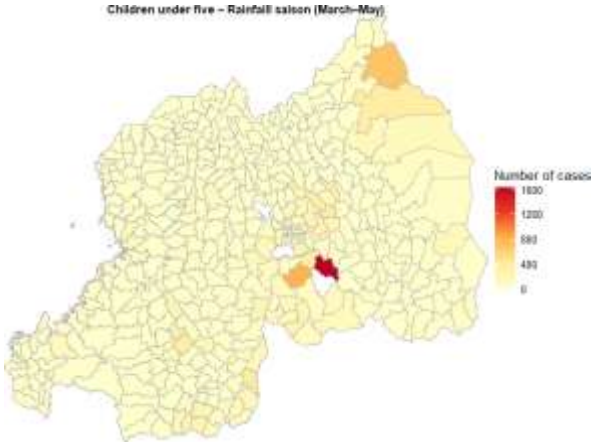

Figure 3: Malaria cases among children under five for the rainy season (March to May)

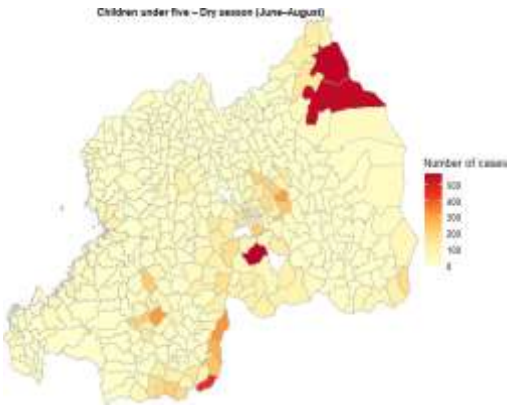

Figure 4: Malaria cases among children under five for the dry season (June to August)

A spatial analysis of malaria cases among children under five during the rainy and dry seasons reveals a consistent and significant seasonal decline.

Case concentrations are observed to be markedly higher during the rainy season (March to May), particularly in eastern and southeastern districts such as Bugesera, Kirehe, Ngoma, and Kayonza. This phenomenon is consistent with the findings of established entomological research, which demonstrates that the rainy season leads to increased availability of breeding sites, enhanced mosquito survival rates, and accelerated parasite development. These factors, when considered collectively, result in an increase in transmission intensity.

In contrast, the dry season (June to August) demonstrates a noticeable decline in malaria cases in most districts. Despite the persistence of residual transmission in select localized regions, the overall intensity has been significantly reduced. This finding indicates that climatic conditions can directly influence the potential for seasonal transmission.

These observations underscore the imperative for malaria control strategies to incorporate seasonality.

While the analysis of malaria among children under five years shows a pronounced seasonal decline, it

is important to examine whether this pattern also applies to other high-risk groups. Pregnant women, for example, may face different exposure conditions or health system interactions.
Compared to children, the spatial distribution of malaria among women during the same periods reveals both similarities and notable differences. The figures below present these maps, which allow us to assess whether the seasonal drop observed in pediatric cases is equally reflected in adult female populations.

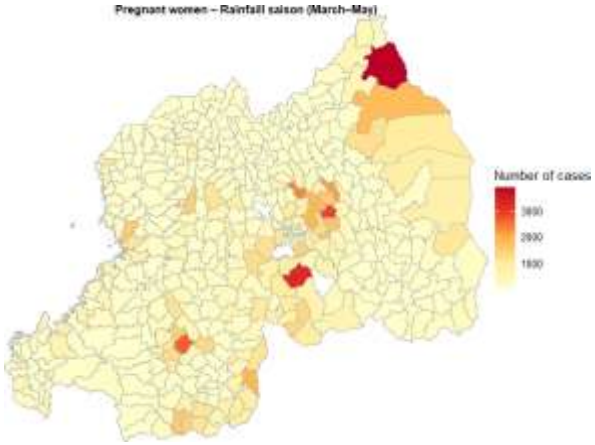

Figure 5: Rainy season (March–May) Malaria cases among pregnant women for the rainy season (March–May)

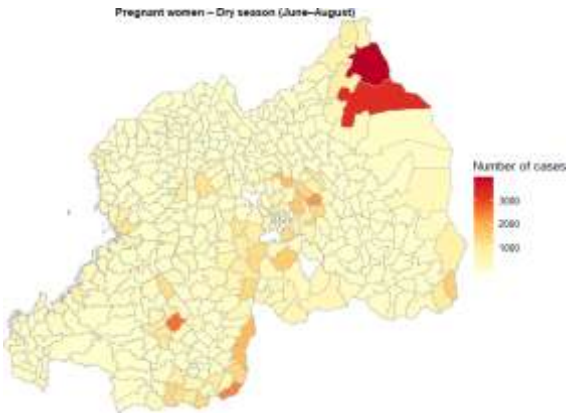

Figure 6: Malaria cases among pregnant women for the dry season (June to August)

The spatial patterns of malaria cases among women display partial overlap with those observed in children under five, particularly during the rainy season (March to May), where high case concentrations appear in northeastern and central districts such as Nyagatare and Muhanga. This finding indicates that both groups are exposed to comparable environmental factors during periods of peak transmission.
However, in contrast to the paediatric maps, where there is a clear decline in case burdens during the dry season (June to August), the reduction in malaria cases among women is less pronounced. It is noteworthy that several districts continue to report substantial case numbers even during the dry season, including Nyagatare and parts of the southeastern region. This persistence could be indicative of different behavioural patterns (e.g. mobility, exposure during agricultural work), gaps in targeted interventions like IPTp, or differences in immunity.

3.2.1. Mosquito lifecycle parameters based on temperature and rainfall

In addition to the spatial distribution of malaria cases, it is imperative to comprehend the biological and ecological mechanisms that underpin transmission in order to anticipate seasonal fluctuations and optimise intervention timing. In the following section, the focus is directed towards an analysis of the climate-sensitive lifecycle of the malaria vector, with particular reference to its implications for transmission potential in Rwanda.
Utilising daily temperature and rainfall data, a simulation was conducted to ascertain the development rates and survival probabilities of mosquitoes across key stages, from egg to adult. The validity of these simulations is contingent upon the utilisation of entomological parameters that have been extracted from a range of extant laboratory and semi-field studies (see White, 2011; Lunde, 2013; and Supplemental White, 2011). The objective of this study is to quantify the impact of environmental fluctuations on mosquito dynamics, and consequently, the influence on malaria risk. Table 3 summarizes the key parameters used in this biological modelling approach.

Table 3: Key entomological parameters used in the temperature- and rainfall-dependent mosquito lifecycle model.

Parameter	Description	Value / Function
δ	Duration of gonotrophic cycle	$3\ days$ [15]
b	Oviposition rate (eggs per mosquito per day)	21.19 [15]
μ_M	Daily mortality rate of adult mosquitoes	$0.096\ day^{-1}$ [15]
μ_P	Mortality rate of pupae	$0.25 day^{-1}$ [15]
d_E, d_L, d_P	Duration of egg, larval and pupal stages	$6.64, 3.72, 0.64\ days$ [16]
μ_E^0, μ_L^0	Baseline mortality of early/late instars	$0.035 day^{-1}$ [16]
γ	Density-dependence modifier (late larvae)	13.25 [15]
$K(t)$	Carrying capacity	Rainfall-based exponential model [15]
τ	Rainfall window affecting $K(t)$	$4\ days$ [15]
$f(T)$	Temperature-dependent dev. rates	fitted functions [15], [16]
$s(T)$	Temperature-dependent survival	fitted functions [15]

3.2.2. Daily temperature and rainfall in Rwanda

Temperature and rainfall have been identified as the most significant environmental factors influencing mosquito population dynamics. In Rwanda, the mean annual temperature remains relatively stable, with

slight increases around days 90 and 250 (late March and early September), and a noticeable dip during the middle of the dry season (around day 190). This thermal stability provides a foundation for year round mosquito survival Rainfall, conversely, displays a distinct bimodal pattern, with peaks occurring around days 90–120 and 270–310, corresponding to Rwanda's two rainy seasons. These periods coincide with increased availability of mosquito breeding sites due to surface water accumulation, and thus with heightened malaria transmission potential. The onset of the dry season, characterised by a pronounced decline in rainfall mid- year, coincides with a contraction of vector populations and a limitation of larval habitats.

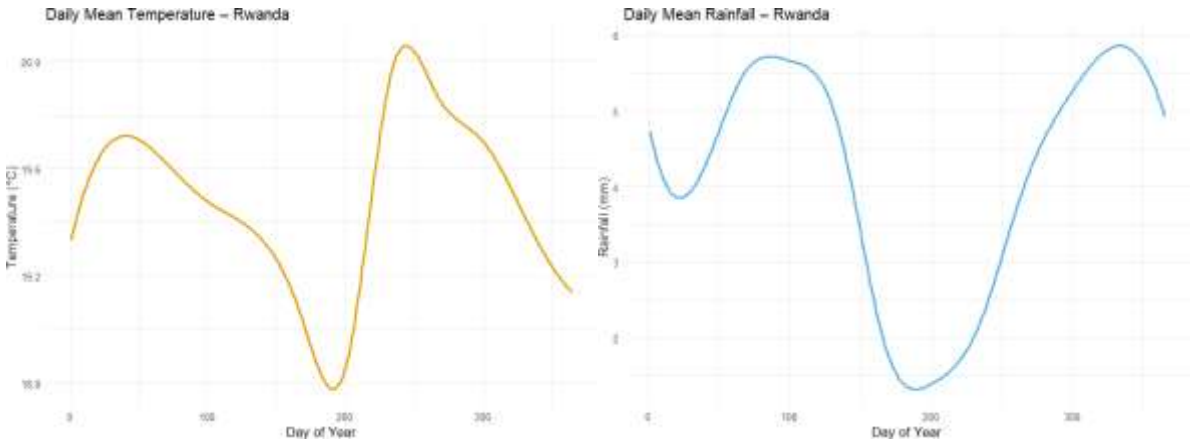

(a) Daily Mean Temperature **(b)** Daily Mean Rainfall

Figure 7: Average daily climatic conditions across Rwanda, based on observed temperature and rainfall patterns.

These climatic signals directly modulate key biological processes in the mosquito lifecycle, and they serve as temporal anchors for the simulation of temperature- and rainfall-dependent transmission parameters. These parameters will be described in the following section.

3.2.3. Mosquitoes lifecycle parameters based on Temperature and rainfall

In order to evaluate the manner in which seasonal climate modulates mosquito biology and malaria transmission potential, a simulation was conducted in which key lifecycle parameters were modelled as functions of both temperature and rainfall. The relationships under discussion are grounded in published entomologi- cal studies, which define development durations as temperature-dependent, and survival and recruitment as jointly influenced by temperature and environmental moisture.

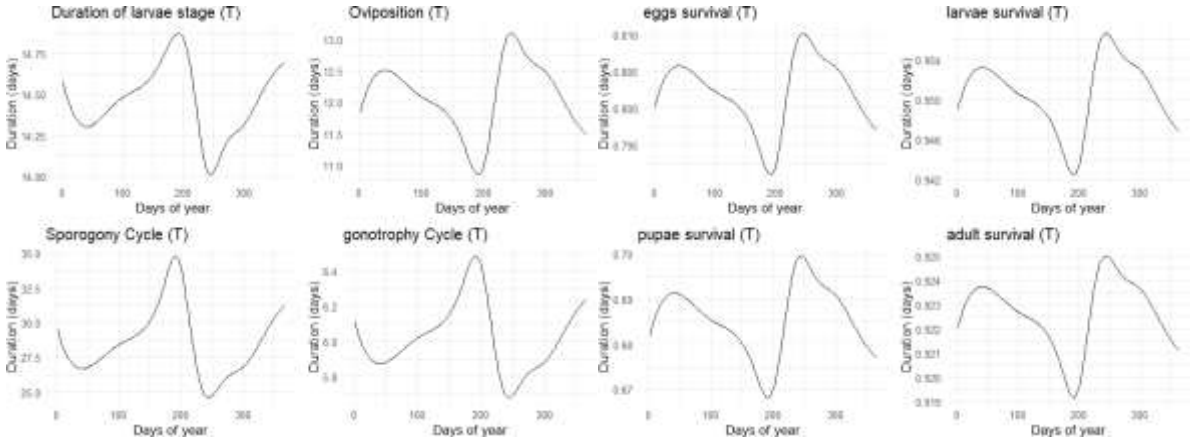

(a) Development and cycle durations **(b)** Survival probabilities by stage

Figure 8: Simulated mosquito lifecycle metrics as a function of daily temperature in Rwanda.

As illustrated in Figure 8, the seasonal progression of both biological cycle durations and stage-specific survival probabilities is demonstrated. The development durations encompassing the larval stage, oviposition, gonotrophic cycle and sporogony are known to lengthen during periods of lower temperature and reduced moisture, a phenomenon that typically occurs around the mid-year dry season. These extended periods are indicative of physiological deceleration in suboptimal conditions, resulting in diminished vector productivity and protracted transmission cycles.

The survival probabilities of the species across all life stages exhibit a similar trend, with a sharp decrease during the driest and hottest parts of the year. This decline is concomitant with elevated environmental stress and constrained access to aquatic breeding habitats. Rainfall is of particular importance in this ecosystem, since it is a key factor in regulating metabolic rates, while temperature is responsible for ensuring habitat availability and humidity levels that are conducive to the persistence of vector species.

It is evident that these climate-driven patterns demonstrate a robust correlation between environmental conditions and the biological potential for malaria transmission. The pronounced seasonal shifts in development and survival support the design of adaptive, climate-aware control strategies that anticipate periods of vector expansion or suppression.

4. Discussion

The objective of this study was to explore the long-term dynamics of malaria transmission under the influence of climate variability. To this end, a stochastic and spatially explicit modelling framework grounded in biological realism was employed. The findings indicate that climatic factors, specifically temperature and rainfall, play a pivotal role in shaping the seasonal progression of the mosquito lifecycle. This, in turn, governs the variable intensity of malaria risk across different geographical locations and temporal periods.

The spatial maps of malaria cases among children and women exhibited a robust seasonal signal, with transmission peaking during rainy periods and waning during the dry season. This pattern is consistent with well-documented epidemiological trends observed across East Africa, where the abundance of breeding sites and ambient humidity drive Anopheles proliferation during the long and short rains . However, while children under five exhibited a marked reduction in cases during the dry months, this was not uniformly observed among women, suggesting differing patterns of exposure, immunity, or access to care. This discrepancy underscores the necessity of conducting a comprehensive risk assessment, taking into account the diverse characteristics of different vulnerable groups, when devising intervention strategies.

The findings were further reinforced by stochastic simulations, which confirmed the observed seasonal effects. In circumstances of reduced recruitment or augmented noise intensity, the vector and infection compartments demonstrated extinction or fade-out, thus exemplifying the vulnerability of transmission under suboptimal climatic conditions. Conversely, simulations under favourable climate conditions demonstrated sustained transmission potential, particularly when both temperature and moisture levels were optimal. These findings are consistent with the theoretical expectations of Ross-Macdonald-type models adapted to climate-dependent parameters (see Smith, 2012; Parham, 2010).

The simulation of biological parameters from empirical temperature and rainfall functions has elucidated the underlying mechanisms of these seasonal dynamics. As demonstrated in Figure 10, the duration of development (e.g., gonotrophic cycle, sporogony) was shortest during the warmest and wettest parts of the year. This supports the hypothesis that accelerated parasite maturation and mosquito reproduction occurred during these periods. Conversely, survival probabilities exhibited a precipitous decline during periods of aridity or extreme temperatures, thereby diminishing the resilience of vector populations. The integration of these temperature- and rainfall-sensitive parameters provides a more detailed and temporally responsive perspective on vector ecology, building upon earlier research that solely considered temperature effects [16, 17]. Notwithstanding the contributions outlined above, the model exhibits several limitations. The spatial structure is predicated on the assumption of homogeneity within districts, yet it does not explicitly incorporate human mobility or vector mobility, both of which are known to influence

transmission heterogeneity [18]. Furthermore, the utilisation of rainfall as a proxy for moisture and habitat availability, without accounting for land use, hydrology, or evapotranspiration, may have resulted in an inaccurate assessment of larval site persistence. The entomological parameters, although derived from robust literature, may not fully capture intra-species variation or local behavioural adaptations among Rwandan vector populations.

Nevertheless, the model's flexibility allows for its extension and calibration with local data. Future research could benefit from the integration of this framework with remote sensing inputs (e.g., NDVI, LST), the incorporation of high-resolution mobility data, and the exploration of intervention strategies using stochastic control or agent-based approaches. It is imperative to acknowledge the capacity to generate dynamic maps of entomological parameters, including the vector recruitment rate. The potential for early warning systems and adaptive control planning in the context of climate change is highlighted by $\theta_M(t)$.

In summary, the present study demonstrates that integrating stochasticity, spatial heterogeneity, and climate-driven biological processes significantly enhances our ability to understand and anticipate malaria transmission dynamics. The substantial seasonal modulation of development and survival that has been observed in the course of the simulations serves to reinforce the necessity for interventions that are climate-adaptive, for spatial targeting, and for continuous monitoring of environmental drivers in regions that are experiencing high levels of burden.

5. Conclusion

The objective of this study was to comprehend the long-term dynamics of malaria transmission by integrating climate variability, biological mechanisms, and spatial patterns into a unified modelling framework. Stochastic simulations and spatial analysis were employed to ascertain the impact of environmental factors, chiefly temperature and rainfall, on the development, survival and, ultimately, the transmission potential of malaria in Rwanda. The findings indicated a robust seasonal pattern, with both biological cycles and disease incidence exhibiting a close correlation with the country's bimodal rainfall pattern. By integrating daily meteorological data with entomological functions, it was demonstrated how shifts in climate conditions shape the viability of vector populations and the risk of sustained transmission.

These findings contribute to a growing body of research that emphasises the importance of environmental context in malaria epidemiology. Whilst earlier models have addressed the impact of temperature on vector competence, this study broadens the perspective by explicitly incorporating both moisture dynamics and stochastic variability. These elements are crucial for understanding transmission in real-world, fluctuating settings. The findings of this study serve to reinforce the theoretical predictions that transmission fades under marginal climatic conditions, thereby underscoring the significance of minor fluctuations in environmental drivers on transmission dynamics.

From a pragmatic perspective, the findings provide significant insights for malaria control programmes seeking to align their strategies with seasonal and spatial transmission patterns. For instance, the model iden- tifies time windows – typically during and just before the rainy seasons when vector recruitment, survival, and parasite development accelerate. These moments represent critical opportunities to scale up vector con- trol interventions, including indoor residual spraying (IRS), the distribution and replacement of long-lasting insecticidal nets (LLINs), and environmental larval source management. Furthermore, the model's structure facilitates the optimisation of intermittent preventive treatment (IPT) for pregnant women and seasonal malaria chemoprevention (SMC) for children, by determining the timing and location of these interventions to maximise their impact.

Moreover, the spatial dimension of the simulations indicates that a one-size-fits-all approach may be inadequate. It is evident that districts exhibiting persistent or less seasonal transmission such as those in eastern Rwanda may require year-round intervention coverage. Conversely, other regions could benefit from more targeted, time limited strategies. This kind of localized, data-driven planning has the potential to enhance resource efficiency and improve outcomes, especially in settings where resources are limited. However, the study is not without its limitations. The spatial model under scrutiny here makes the assumption of internal homogeneity, whilst eschewing any explicit accounting for human mobility, intervention coverage, or socio-economic variation. The utilisation of literature based entomological

parameters, while founded on empirical evidence, may not wholly mirror local vector behavior or ecology. It is recommended that future endeavors seek to validate and calibrate the model with field data, integrate real-time environmental indicators (e.g., satellite derived water indices), and explore predictive applications such as early warning systems or intervention scenario testing.

In conclusion, this study proposes a framework that captures the complex, climate-sensitive nature of malaria transmission. This finding serves to reinforce the prevailing view that transmission is not solely a biological phenomenon, but also an environmental process, which can be anticipated, disrupted, and ultimately controlled. By aligning interventions with ecological signals, we move closer to a future where malaria transmission is not only understood but strategically outmaneuvered.

References

[1] J. Talapko, I. Š krlec, T. Alebi´c, M. Juki´c, A. V˘cev, Malaria: The past and the present (jun 2019).
[2] J. M. Marshall, C. E. Taylor, Malaria control with transgenic mosquitoes, PLoS medicine 6 (2) (2009) e1000020.
[3] W. H. Organization, et al., World malaria report 2024: addressing inequity in the global malaria response (2024).
[4] W. H. Organization, World malaria report 2023, World Health Organization, 2023.
[5] R. Ross, The prevention of malaria, John Murray, 1911.
[6] M. G. Macdonald. G, The epidemiology and control of malaria. (1957).
[7] L. J. White, R. J. Maude, W. Pongtavornpinyo, S. Saralamba, R. Aguas, T. Van Effelterre, N. P. Day, N. J. White, The role of simple mathematical models in malaria elimination strategy design, Malaria journal 8 (2009) 1–10.
[8] S. Mandal, R. R. Sarkar, S. Sinha, Mathematical models of malaria-a review, Malaria journal 10 (2011) 1–19.
[9] E. Ndamuzi, P. Gahungu, Mathematical modeling of malaria transmission dynamics: case of burundi, Journal of applied mathematics and physics 9 (10) (2021) 2447–2460.
[10] D. Wanduku, A comparative stochastic and deterministic study of a class of epidemic dynamic models for malaria: exploring the impacts of noise on eradication and persistence of disease, arXiv preprint arXiv:1809.03897 (2018).
[11] L. Wang, Z. Teng, C. Ji, X. Feng, K. Wang, Dynamical behaviors of a stochastic malaria model: a case study for yunnan, china, Physica A: Statistical Mechanics and its Applications 521 (2019) 435–454.
[12] P. V. Le, P. Kumar, M. O. Ruiz, Stochastic lattice-based modelling of malaria dynamics, Malaria journal 17 (2018) 1–17.
[13] S. B. Affognon, H. E. Tonnang, P. Ngare, B. K. Kiplangat, S. Abelman, J. K. Herren, Optimizing microbe-infected mosquito release: a stochastic model for malaria prevention, Frontiers in Applied Math- ematics and Statistics 10 (2024) 1465153.
[14] P. Van den Driessche, J. Watmough, Reproduction numbers and sub-threshold endemic equilibria for compartmental models of disease transmission, Mathematical biosciences 180 (1-2) (2002) 29–48.
[15] M. T. White, J. T. Griffin, T. S. Churcher, N. M. Ferguson, M.-G. Bas ´añez, A. C. Ghani, Modelling the impact of vector control interventions on anopheles gambiae population dynamics, Parasites & vectors 4 (2011) 1–14.
[16] T. M. Lunde, M. N. Bayoh, B. Lindtjørn, How malaria models relate temperature to malaria transmis- sion, Parasites & vectors 6 (2013) 1–10.
[17] E. A. Mordecai, K. P. Paaijmans, L. R. Johnson, C. Balzer, T. Ben-Horin, E. de Moor, A. McNally, S. Pawar, S. J. Ryan, T. C. Smith, et al., Optimal temperature for malaria transmission is dramatically lower than previously predicted, Ecology Letters 16 (1) (2013) 22–30.
[18] N. W. Ruktanonchai, P. DeLeenheer, A. J. Tatem, V. A. Alegana, T. T. Caughlin, E. Erbach-Schoenberg, C. Louren ¸co, C. Pezzulo, K. Nilsen, C. W. Ruktanonchai, et al., Identifying malaria transmission foci for elimination using human mobility data, PLoS Computational Biology 12 (4) (2016) e1004846.
[19] X. Mao, Stochastic differential equations and applications, Elsevier, 2007.

Appendix A. Proofs of Theoretical Results

Appendix A.1. Positivity of the system

Proof. To ensure positivity, we apply Itô's Lemma to the logarithm of each variable. Define:

$$Y = \ln X, \quad \text{where } X \in \{S_M, I_M, S_H, I_H, R_H\} \quad (A.1)$$

Using Itô's formula for a function $h(X) = \ln X$, we obtain:

International Journal of Environmental Sciences
ISSN: 2229-7359
Vol. 11 No. 14s, 2025
https://www.theaspd.com/ijes.php

$$d(\ln X) = \frac{1}{X}\, dX - \frac{1}{2}\frac{\left(g(X)\right)^2}{X^2}\, dt \quad (A.2)$$

- Positivity of S_M

Applying Ito's lemma to $Y = ln(S_M)$

$$d(\ln S_M) = \frac{1}{S_M}\, dS_M - \frac{1}{2}\frac{(\sigma_{SM} S_M)^2}{S_M^2}\, dt \quad (A.3)$$

Substituting $d(S_M)$:

$$d(\ln S_M) = \frac{\lambda_M}{S_M} - \beta_{MH} I_H - \mu_M - \frac{1}{2}\sigma_{SM}^2\, dt + \sigma_{SM}\, dW_1 \quad (A.4)$$

Since the drift term does not force S_M to zero and the noise term vanishes at zero, S_M remains strictly positive.

- Positivity of I_M

Applying Itô's Lemma to $Y = ln(I_M)$:

$$d(\ln I_M) = \frac{\beta_{MH} S_M I_H}{I_M} - \mu_M - \frac{1}{2}\sigma_{IM}^2\, dt + \sigma_{IM}\, dW_2 \quad (A.5)$$

Since $\frac{\beta_{MH} S_M I_H}{I_M} \geq 0$ and the noise term vanishes at zero, I_M remains positive.

- Positivity of S_H

Applying Itô's Lemma to $Y = ln(S_H)$:

$$d(\ln S_H) = \frac{\lambda_H}{S_H} - \beta_{HM} I_M - \mu_H + \frac{\gamma R_H}{S_H} - \frac{1}{2}\sigma_{SH}^2\, dt + \sigma_{SH}\, dW_3 \quad (A.6)$$

Since the drift term does not force S_H to zero and the noise term vanishes at zero, S_H remains strictly positive.

- Positivity of I_H

Applying Itô's Lemma to $Y = ln(I_H)$:

$$d(\ln I_H) = \left(\frac{\beta_{HM} S_H I_M}{I_H} - (\mu_H + \rho) - \frac{1}{2}\sigma_{IH}^2\right) dt + \sigma_{IH}\, dW_4 \quad (A.7)$$

Since $\frac{\beta_{HM} S_H I_M}{I_H} \geq 0$ and the noise terms vanishes at zero, I_H remains strictly positive.

- Positivity of R_H

Applying Itô's Lemma to $Y = ln(R_H)$:

$$d(ln\, R_H) = \left(\frac{\rho I_H}{R_H} - (\mu_H + \gamma) - \frac{1}{2}\sigma_{RH}^2\right) dt + \sigma_{RH}\, dW_5 \quad (A.8)$$

Since $\frac{\rho I_H}{R_H} \geq 0$ and the noise terms vanishes at zero, R_H remains strictly positive.

Appendix A.2. Stability Analysis

Proof. To analyze the stability of the system, we first determine the equilibrium points by setting the drift terms to zero:

$$\lambda_M - \beta_{MH} S_M I_H - \mu_M S_M = 0 \quad (A.9)$$
$$\beta_{MH} S_M I_H - \mu_M I_M = 0 \quad (A.10)$$
$$\lambda_H - \beta_{HM} S_H I_M - \mu_H S_H + \gamma R_H = 0 \quad (A.11)$$
$$\beta_{HM} S_H I_M - (\mu_H + \rho) I_H = 0 \quad (A.12)$$
$$\rho I_H - (\mu_H + \gamma) R_H = 0 \quad (A.13)$$

- Local Stability Analysis

We compute Jacobian matrix J evaluated at an equilibrium point $(S_M^*, I_M^*, S_H^*, I_H^*, R_H^*)$. The Jacobian is given by:

$$J = \begin{bmatrix} -\beta_{MH} I_H - \mu_M & 0 & 0 & -\beta_{MH} S_M & 0 \\ \beta_{MH} I_H & -\mu_M & 0 & \beta_{MH} S_M & 0 \\ 0 & -\beta_{HM} S_H & -\beta_{HM} I_M - \mu_H & 0 & \gamma \\ 0 & \beta_{HM} S_H & \beta_{HM} I_M & -(\mu_H + \rho) & 0 \\ 0 & 0 & 0 & \rho & -(\mu_H + \gamma) \end{bmatrix}. \quad (A.14)$$

The stability is determined by the eigenvalues of J. If all eigenvalues have negative real parts, the equilibrium is locally asymptotically stable.

Theorem A.1. The stochastic epidemic model is stochastically asymptotically stable in the mean square sense if there exists a positive definite Lyapunov function $V(S_M, I_M, S_H, I_H, R_H)$ such that the infinitesimal generator LV satisfies:

$$LV \leq -cV + d \quad (A.15)$$

for some positive constants c and d. Moreover, for stability, the noise intensity parameters $\sigma_{SM}, \sigma_{IM}, \sigma_{SH}, \sigma_{IH}, \sigma_{RH}$
must satisfy certain bounded conditions such that stochastic perturbations do not dominate the deterministic stability properties.

- Global Stability Analysis

We construct a suitable Lyapunov function V and analyze its time derivative dV/dt to establish global stability. Define:

$$V = a_1(S_M - S_M^*)^2 + a_2(I_M - I_M^*)^2 + a_3(S_H - S_H^*)^2 + a_4(I_H - I_H^*)^2 + a_5(R_H - R_H^*)^2 \quad (A.16)$$

Computing dV/dt and ensuring dV/dt ≤ 0 establishes global stability.

Appendix A.3. Extinction of the disease

Proof. Let define $Z(t) = \ln I_H(t)$.

Since $I_H(t) > 0$ almost surely, Z(t) is therefore well defined. Now let's apply Itô's formula:

$$\text{Since} I_H(t) > 0 \text{almost surely, } Z(t) \text{is therefore well defined. Now let's apply Itô's formula:}$$

$$dZ(t) = \frac{1}{I_H(t)} dI_H(t) - \frac{1}{2I_H(t)^2} \left(dI_H(t)\right)^2.$$

$$\text{Using the SDE of } I_H(t), \text{ we compute:}$$

$$\frac{1}{I_H} dI_H = \left(\frac{\beta_{HM} S_H I_M}{I_H} - (\mu_H + \rho) \right) dt + \sigma_{IH} dW_t,$$

$$(dI_H)^2 = \sigma_{IH}^2 I_H^2 dt \quad \Rightarrow \quad \frac{1}{2I_H^2} (dI_H)^2 = \frac{1}{2} \sigma_{IH}^2 dt.$$

$$dZ(t) = \left(\frac{\beta_{HM} S_H I_M}{I_H} - (\mu_H + \rho) - \frac{1}{2} \sigma_{IH}^2 \right) dt + \sigma_{IH} dW_t.$$

Using the assumption $\frac{S_H I_M}{I_H} \leq \delta$, so: $\frac{\beta_{HM} S_H I_M}{I_H} \leq \beta_{HM} \delta$. Thus,

$$dZ(t) \leq \left(\beta_{HM} \delta - (\mu_H + \rho) - \frac{1}{2} \sigma_{IH}^2 \right) dt + \sigma_{IH} dW_t.$$

$$\text{Define} \lambda = \frac{1}{2} \sigma_{IH}^2 - (\mu_H + \rho) + \beta_{HM} \delta. \text{ Under the assumption } \lambda > 0, \text{ we obtain:}$$

$dZ(t) \leq -\lambda dt + \sigma_{IH} dW_t$. Integrating both sides:

$$Z(t) \leq Z(0) - \lambda t + \sigma_{IH} W_t.$$

$$\text{Dividing by } t \text{ and using the strong law of large numbers for Brownian motion:}$$

$$\limsup_{t \to \infty} \quad \frac{Z(t)}{t} \leq -\lambda \quad \text{almost surely.}$$

$$\text{Since} Z(t) = \ln I_H(t), \text{ we conclude:}$$

$$\limsup_{t \to \infty} \quad \frac{1}{t} \ln I_H(t) \leq -\lambda, \quad \text{almost surely.}$$

Remark. This result shows that under low transmission conditions ($R_0 < 1$) and moderate noise intensity, infection in the human population will vanish with probability one. The decay is exponential, meaning that the disease not only fades, but does so rapidly and reliably over time, reinforcing the impact of both deterministic control and environmental variability.

Appendix A.4. Stationary

Proof. Let $V(X) = |X|^2 = \sum x_i^2$.

$$\text{Then } \nabla V = 2X, \quad \nabla^2 V = 2I.$$

The generator is

$$LV = 2\langle X, b(X) \rangle + 2 \sum \sigma_i^2 x_i^2$$

Since each $x_i b_i(X)$ includes negative quadratic terms, there exist constants a > 0, C > 0 such that

$$\langle X, b(X) \rangle \leq -a|X|^2 + C$$

Hence

$$LV \leq -2a\,|X|^2 + 2C + 2\sigma^2_{\{\max\}}|X|^2.$$
$$\text{Let } c := 2a - 2\sigma^2_{\{\max\}} > 0, \text{then}$$
$$LV \leq -c\,|X|^2 + d.$$

By the Theorem 4.6 of Mao (2007) [19], this implies existence of a stationary distribution.
Remark. This means that when the basic reproduction number R0 is more than 1 and the noise intensity is not too large, the disease will continue in the population. In other words, the state variables change randomly over time but stay within a biologically meaningful range in R^5, and the system's long-term behavior is probabilistic.

Appendix A.5. Ergodicity

Proof. Define:

$V_1 = \sigma_{\{SM\}S_M}\partial_{\{S_M\}}$, $V_2 = \sigma_{\{IM\}I_M}\partial_{\{I_M\}}$, $V_3 = \sigma_{\{SH\}S_H}\partial_{\{S_H\}}$, $V_4 = \sigma_{\{IH\}I_H}\partial_{\{I_H\}}$, $V_5 = \sigma_{\{RH\}R_H}\partial_{\{R_H\}}$, $V_0 = b(X)$.

Compute Lie brackets:

$$[V_0, V_i](X) \neq 0 \quad \text{for } i = 1, \ldots, 5,$$

due to nonlinear interaction terms.
Let L(X) be the Lie algebra generated by $\{V_1, \ldots, V_5\}$ and their brackets with V_0. Then:

$$\text{Rank}\big(L(X)\big) = 5 \text{ for all } X \in R^{\{5\}}_{\{+\}} \setminus K$$

By Hörmander's theorem, the process is hypoelliptic. Combined with positivity and the existence of a Lyapunov function, ergodicity follows.

Remark. The ergodicity result means that, in the right conditions, the malaria transmission system will forget its initial state and evolve towards a stable long-term statistical behavior. This means that, over time, the probability distribution of the disease states will come to the same average, even though the environment changes randomly.